WICKING OPTIMIZATION FOR THERMAL COOLING -WITH A TITANIUM BASED HEAT PIPE SYSTEM

C. Ding[1], P. Bogorzi[2], M. Sigurdson[2], C.D. Meinhart[2] and N.C. MacDonald[2]*
[1]California Nanosystems Institute, UCSB, Santa Barbara, CA, USA
[2]Department of Mechanical Engineering, UCSB, Santa Barbara, CA, USA

ABSTRACT

Micromachined titanium pillars with nanoscale tiania structures on surfaces are adopted to form wicking material for a proposed flat heat pipe system. This unique bitextured titania structure (BTS) provides a suprerhydrophilic surface and improves the wicking ability of the titanium based pillar arrays. Experimental studies on optimizing the wicking behaviors of BTS pillar arrays are reported in this work. Oxidization and plating techniques are applied to modify the surface properties and pillar/gap dimensions of the wicks. A titanium based flat heat pipe is proposed to integrate the BTS wicks and study the concept of this titanium based flat heat pipe architecture. A thermal conductivity ~500W/m-K (with contact resistance included) is achieved at around 118°C. The chamber of this Ti heat pipe is formed by hermetically welding two substrates together using laser welding technique. The hermiticity performance of the chamber is studied with helium leaking approaches. A leaking rate of 3.4×10^{-10} atm.cm^3/s is achieved for a chamber of ~170μL in volume.

INTRODUCTION

Flat Titanium Heat Pipe Architecture

Flat heat pipes adopt a relatively much larger geometry in planar direction than traditional heat pipes to provide a potential for transporting or spreading a large amount of heat. They are finding their ways in the thermal cooling systems for applications such as computer chips, circuit boards, and space based radar systems which consume a high density of power. A flat heat pipe has wicking materials on the interior walls of its chamber to automatically pump the cooling fluids from the heat sink side to the evaporator side when transporting heat. The wicking materials enable heat pipes some unique functions that thermal siphons could not achieve [1]. The flat geometry allows micro/nano-scale machining techniques to be applied for forming unique wicking materials such as carbon nanotubes, sintered copper, micromachined structures, etc..

Besides wicking materials flat heat pipes have two other important components: a hermetically-sealed cavity and a working fluid. The cavity must be hermetically sealed to avoid input of any noncondensable gases by leaking. Ideally, only different phases of a working fluid are allowed in the chamber. The merit number is used to select a working fluid [2] in Anderson's work for heat pipe systems. In this work water is adopted as the working fluid.

During operation, heat is applied to the hot side of a wicking substrate, causing evaporation. The water vapor is transported to a cold region and condensed by rejecting heat with a heat sink. The condensed water is then pumped back to the evaporating region by the wicking material which provides capillary force when contacting with working fluids. This process is continuous forming different steady states during operations. Figure 1 shows the schematic of a laser-welded titanium flat heat pipe architecture. Fabrication of the device will be described in the latter part of this paper. This device is enhanced by adding the Ti posts to support the relatively thin sealing substrate, which avoids the volume changes when chamber pressure is lower than the outside pressure.

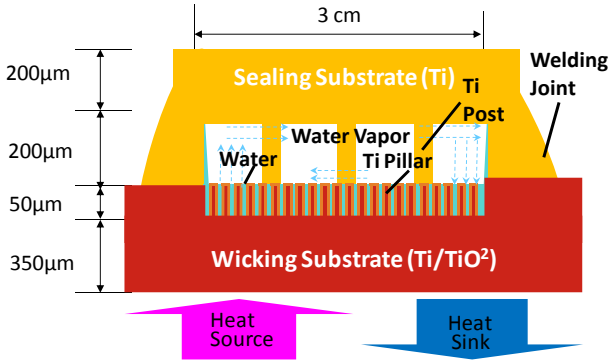

Figure 1: Schematic of the titanium based flat heat pipe. Note that the Ti posts function as supporting structure for the sealing substrate.

Wetting on Textured Surfaces

The following Wenzel equation [3], predicts that rough surfaces possibly help enhance the wettability of high energy solid surfaces, where *r* is the roughness number defined in Figure 2.

$$\cos\theta_e^r = r\cos\theta_e \quad (1)$$

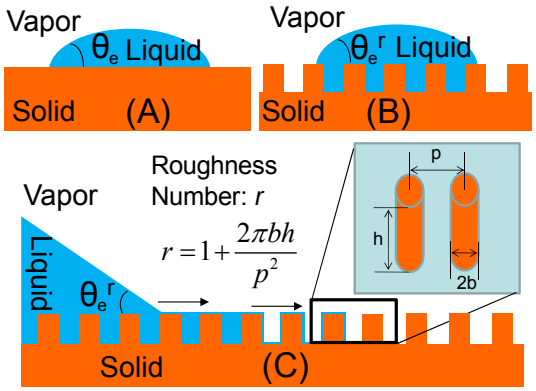

Figure 2: Flow of the impregnating film at the front boundary. Figure A shows the Young's contact angle; Figure B and C show the static and dynamic cases of the wetting on solid surfaces.

However the rough surfaces help with wetting only when the contact angle (shown in Fig. 2A) is less than π/2. For a droplet to sit on a smooth and flat surface, the contact angle is governed by the Young's equation:

$$\cos\theta_e = \frac{\gamma_{SV} - \gamma_{SL}}{\gamma} \quad (2)$$

where θ_e is the equilibrium contact angle, γ_{SV}, γ_{SL}, and γ, are the interface energy at the solid-vapor, solid-liquid, and

liquid-vapor interfaces, respectively. For the hydrophilic case, $\theta_e < \pi/2$.

If Young's contact angle is larger than π/2, the roughness will increase the apparent contact angle, leading to superhydrophobic/super-antiwetting case [4]. Since the roughness modifies the value of apparent contact angle superwetting can be achieved by tuning the roughness. For the complete wetting case, the contact angle, θ_e^r, will decrease to zero once the fluid fully wets the wick structure. Our idea is to make micromachined pillars to obtain large surface roughness and optimize the wetting by modifying the pillar dimensions. We denote such a mono-textured surface by its pillar density ϕ_s and roughness r. Provided that the case of wetting as in Fig. 2, the pillars guide water liquid among the arrays and form in a phenomenon similar to wicking but more accurately hemiwicking which is intermediate between spreading and imbibition [5].

The wicking material is usually designed to provide high capillary force on the spreading liquid. The capillary force, $F=\gamma(r-1)$, can be derived using virtual energy method where γ is the surface tension of the wicking fluid. Detailed studies and discussions about wicking dynamics of fluid on textured structured can be found in previous works [5-7]. Although capillary can be well defined, the friction force between fluid and solid surfaces is relatively difficult of measure and analytically define for complicated structures.

FABRICATION

Different kinds of materials such as carbon nanotubes [8], nanowires, sintered copper [9], and micromachined channels have been investigated as wicking materials. In this work, we adopt recently developed titanium bulk micromachining techniques [10] to fabricate titanium pillar arrays as wicking materials, then we modify the micromachined pillars to form micro-&nano-textured (bitextured) titania structures (BTS) (Fig. 3) on all surfaces.

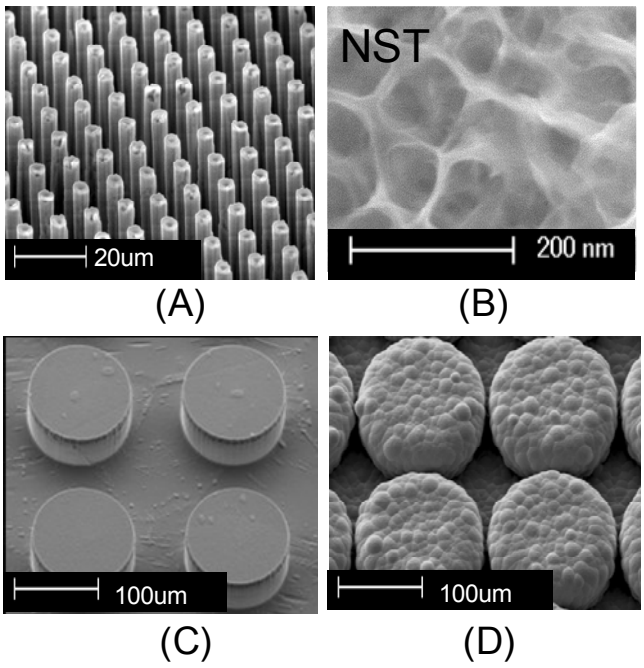

Figure 3: SEM photograph of the 5μm/5μm(Dia./Gap) BTS and 100μm/50μm (Dia/Gap) BTS. All pillars are ~50μm high. The nanostructured titania (NST, Fig. 3B) covers all the pillar surfaces and the bottom floor on Fig. 3A and Figure 3C. Figure 3D shows the SEM photograph of Figure 3C after gold plating.

Two dimensions were fabricated with radius/gap of 5μm/5μm and 100μm/50μm. Further, we modified the surfaces of both dimensions to form BTS. Then we plated gold (Fig. 3D) on the 100μm/50μm arrays to tune the dimensions and formed ~145μm/5μm surfaces to tune the structure dimensions and their wetabilities. Detailed fabrication about bulk micromachining of the Ti pillar arrays and BTS formation can be found in [11].

WETTING EXPERIMENTS FOR OPTIMIZATION

The experiments were done by bringing a drop of water (~40μL) into contact with our samples. Then the flows were recorded with a camera (Nikon D90). The wetting results show all samples are completely wettable with DI water. The recorded video was decomposed to study the travel distance of the front boundary radial path (x) of the spreading water as a function of time (t).

$$x^2=Dt \qquad (3)$$

A curve of the form equation 3 inspired by Washburn equation [12], is well fitted to the collected distance-vs-time data shown in Fig. 4, where D is defined to be dynamic coefficient.

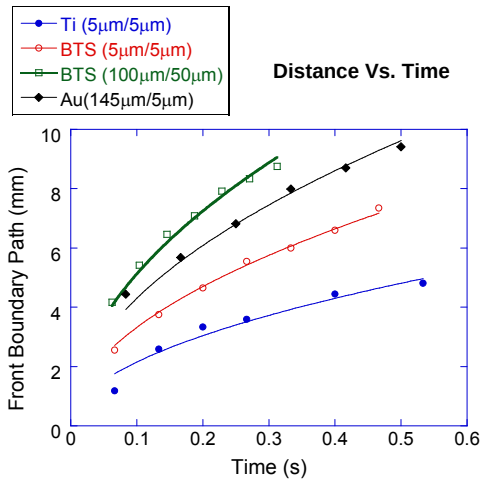

Figure 4: The front boundary flow path vs. time of the four experiments.

The experimental data generate the dynamic coefficients for different wetting experiments listed in Table 1. We proposed to use the velocity profiles as shown in Figure 4 for wicking material performance/design.

Table 1: Dynamic coefficient comparison.

Items	Ti Only 5μm/5μm	BTS 5μm/5μm	BTS 100μm /50 μm	BTS/Au 145μm /5 μm
SQRT(D) ($m/s^{1/2}$)	6.5E-3	1.05E-2	1.62E-2	1.36E-2
D/2 (m^2/s)	2.12E-5	5.50E-5	1.31E-4	9.25E-5

The Velocity-Vs-Distance profile is found by differentiating the fitted curve, $x^2=Dt$, to be:

$$\frac{dx}{dt} = \frac{D}{2}\frac{1}{x} \qquad (3)$$

Equation (3) shows similar diffusive spreading behavior predicted by Washburn equation. Figure 5 shows the compared corresponding velocity profiles by plotting the derived fitting curves from Fig. 4. The super wetting ability of BTS wicking materials not only improve thermal conductivity, but may also help avoid dry-out phenomena of heat pipes.

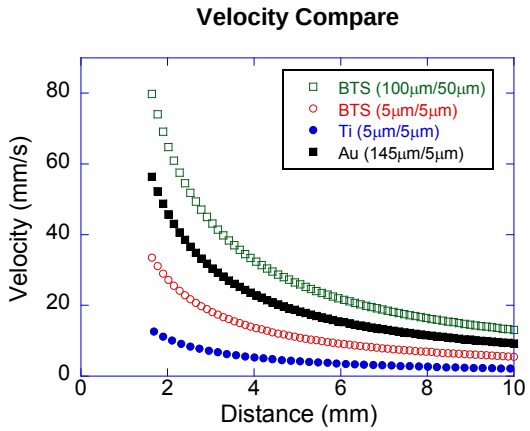

Figure 5: Comparison of the velocity profiles. The wetting (in radius direction) is much faster at the very beginning.

From Fig. 5 it shows that pillar arrays with BTS (100μm/50μm, Dia./Gap) has the fastest traveling speed comparing to all the other three wicking materials. This indicates that wicking materials can be designed and/or modified to provide a broad range of wetting speeds for the wicking needs of micro-fluid based pumping systems. Also these wicking materials provide different capillary limits when heated at elevated temperature. From the experimental studies shown in Fig. 5 we decide to integrate the wicking material shown in Fig. 3C for its fastest wetting speed into the proposed flat titanium heat pipe shown in Fig. 1.

PACKAGING AND THERMAL PERFORMANCE

To investigate the thermal performance of the proposed heat pipe device we packaged two separate substrates (sealing substrate and wicking substrate) as shown in Fig. 1 using a pulsed wave YAG laser welder (Neodymium-Doped Yttrium Aluminum Garnet, Nd: Y3Al5O12) with a wavelength of 1064nm. The bottom substrate contains the wicking material as shown in Fig. 3C with an area of 3cmx3cm. The top substrate has a cavity (200μmx3cmx3cm) with 16 Ti posts evenly located on it for supporting purposes. The net volume of cavity is 170μL. Two charging tubes were welded onto the device with laser welding techniques. The device is then purged with pressurized water vapor for 15minute to eliminate the air inside the device. Then it was charged with ~40μL water so that the water level is about ~10μm above the pillar top surface. The final packaged device is shown in Fig. 6.

The device was tested with one side (0.5cmx3cm) to contact with heat source (copper block) and the other side (1cmx3cm) to contact with a heat sink (thermal electric cooler) via (copper block). Both copper blocks were brought into contact with the device via a thermal interface material (Arctic Silver 5). And the heat flow was monitored by two thermocouples at each copper block to confirm if the system is at steady state.

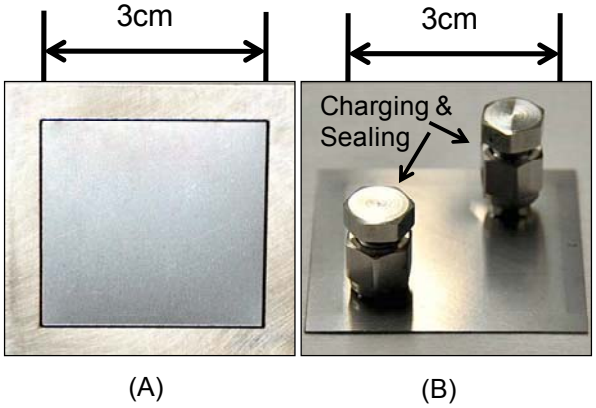

Figure 6: Laser welded Ti heat pipe with Figure (A) as backside and Figure (B) as front side where the two 1/8" charging tubes are sealed with Swagelok end caps.

A copper plane with similar dimensions was used to calibrate the measurement system. A maximum of conductivity 500.085W/m-K (with contact resistance included) was achieved with a steady state heat flow of 8.65W at 118°C on the heat source side of the heat pipe (shown in Fig. 6). Contact area and thermal interface material thickness were measured for calculation of the thermal contact resistances of the interface material. Assuming that the thermal contact resistances at different temperatures are the same then we get the above plot in Fig. 7 as the device thermal conductivity performance which gives a peak performance of ~700W/m-K at 118°C with the heat flow of 8.65W.

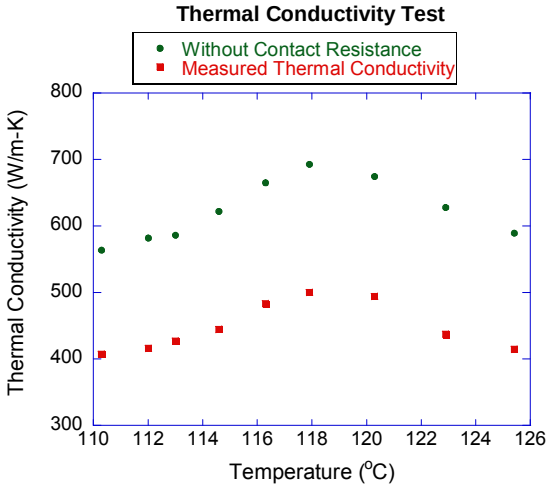

Figure 7: Thermal performance of the flat Ti heat pipe.

HERMITICITY TEST

The titanium heat pipe architecture not only offers rigid, compatible [13] and light weight [14] building structure, but also provides the convenience of packaging at large scale thanks to the weldability of titanium substrates. The hermiticity research in this work was conducted by helium leaking rate test method based on MIL-STD-883E standard. The helium leak detector was used in this test is ASM 142 with a sniffing unit, and its minimum detectable helium leak rate is $1x10^{-11}$atm.cm^3/s. As shown in the schematic (Fig. 8) the test is conducted at room temperature while the pressure is maintained to be 1atm in the test chamber.

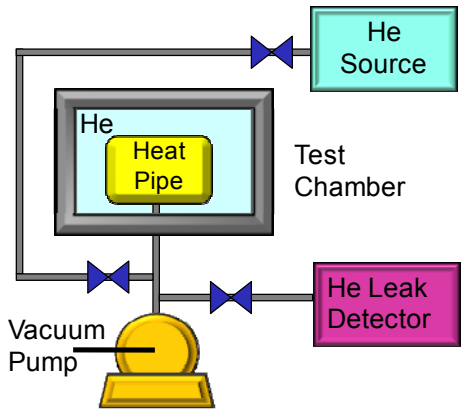

Figure 8: Schematic of hermiticity test with the helium leaking approach.

A device is made (shown in Fig. 9) with the same dimension as Fig. 6 for hermiticity test. The volume under leaking test device is ~170μL with a 1/8 inch outside diameter tube to connect with the adaptors of the test instrument. The device is placed inside of a helium gas chamber with the temperature and pressure inside of the chamber set up to be 23°C and 1atm, respectively. The device is pumped down to create a negative pressure in the cavity. A mass spectrometer is connected to the cavity to measure penetrated helium molecules from the outside chamber into the sealed cavity. The response time to detect helium molecules of ASM 142 leak detector machine is less than a second. In this work the pressure inside of the cavity was pumped down to 0.05 mbar, and the leaking test was carried out three times on same pressure and temperature to investigate consistency of leaking rate. In all three runs after 2 minutes the leaking rate of $3.4x10^{-10}$atm.cm^3/s was measured.

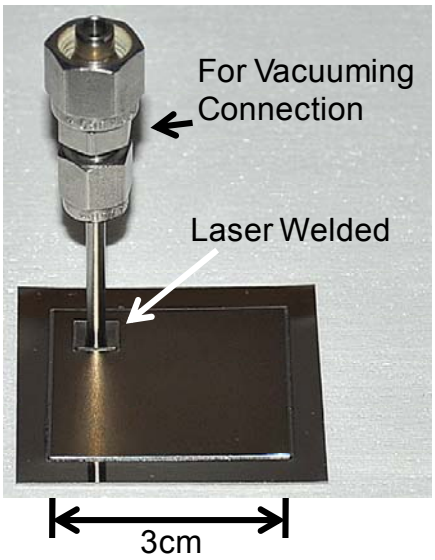

Figure 9: Laser welded device for hermiticity test. The device connects to the testing instrument by a 1/8 inch tube which is laser welded to the heat pipe.

CONCLUSION

Dimensions and surface nanostructures were found to play critical roles on wetting with bitextured tiania structures. The nanostructured titania greatly enhanced the wetting speed for the 5μm/5μm pillar array. However the 100μm/50μm array shows much higher wicking speed than the former wick. Balancing the driving force with the viscous force, the dynamic behavior of the flow on rough solids is found to be diffusive and follows Washburn relation[15]. A thermal conductivity over 500W/m-K (with contact resistance included) is achieved at around 118°C. The chamber of this Ti heat pipe is formed hermetically by welding two substrates together using laser welding technique. The hermiticity performance of the chamber is studied with helium leaking approaches. A leaking rate of $3.4x10^{-10}$ atm.cm^3 /s is achieved for the chamber with a volume of ~170μL.

REFERENCES

[1] P. D. Dunn and D. A. Reay, "Heat pipe," Physics in Technology, vol. 4, pp. 187-201, 1973.
[2] W. G. Anderson, J. H. Rosenfeld, D. Angirasa, and Y. Me, "Evaluation of Heat Pipe Working Fluids in the Temperature Range 450 to 700 K," Space Technology and Applications International Forum (STAIF-04), edited by M. S. El-Genk, American Institute of Physics, Melville, New York, pp. 20-27, 2004.
[3] R. N. Wenzel, "RESISTANCE OF SOLID SURFACES TO WETTING BY WATER," Industrial & Engineering Chemistry, vol. 28, pp. 988-994, 1936.
[4] X. Feng and L. Jiang, "Design and creation of superwetting/antiwetting surfaces," Adv. Mater, vol. 18, pp. 3063-78, 2006.
[5] D. Quéré, "Wetting and Roughness," Annual Review of Materials Research, vol. 38, pp. 71-99, 2008.
[6] J. Bico, U. Thiele, and D. Quéré, "Wetting of textured surfaces," Colloids and Surfaces A: Physicochemical and Engineering Aspects, vol. 206, pp. 41-46, 2002.
[7] C. Ding, G. Soni, P. Bozorgi, C. D. Meinhart, and N. C. MacDonald, "Wicking Study of Nanostructured Titania Surfaces for Flat Heat Pipes," in Nanotech Conference & Expo, Houston, TX, 2009.
[8] U. Vadakkan, G. M. Chrysler, J. Maveety, and M. Tirumala, "A Novel Carbon Nano Tube based Wick Structure for Heat Pipes/Vapor Chambers," in Semiconductor Thermal Measurement and Management Symposium, 2007. SEMI-THERM 2007. Twenty Third Annual IEEE, 2007, pp. 102-104.
[9] L. Mariana, L. O. Radu, S. Gheorghe, L. Magdalena Valentina, and K. Wilhelm, "Metallic Porous Parts for Electronics Devices Cooling," in Electronics Systemintegration Technology Conference, 2006. 1st, 2006, pp. 343-346.
[10] M. P. Rao, M. F. Aimi, E. R. Parker, and N. C. MacDonald, "Single-mask, high aspect ratio, 3D micromachining of bulk titanium," 18th IEEE International Conference on MEMS 2005, pp. 64-67, 2005.
[11] C. Ding, G. Soni, P. Bozorgi, B. Piorek, C. D. Meinhart, and N. C. MacDonald, "A Titanium Based Flat Heat Pipe," in International mechanical engineering congress and exposition, Boston, Massachusetts, 2008.
[12] E. W. Washburn, "The Dynamics of Capillary Flow," Physical Review, vol. 17, p. 273, 1921.
[13] W. Anderson, P. Dussinger, R. Bonner, and D. Sarraf, "High temperature titanium-water and Monel-Water heat pipes," 2006, pp. 2006-4113.
[14] M. Ishizuka, T. Sasaki, and Y. Miyazaki, "Development of Titanium Heat Pipes For Use In Space," 1985, pp. 157-165.

CONTACT
*C. Ding. Public, tel: +1-805-893-5341;
changsong_ding@yahoo.com